Key Points:
- Temperatures and salinities have been reconstructed in the Nordic Seas for Marine Isotope Stage 11
- A cold, low-salinity, buoyant surface water layer persisted in the Nordic Seas during this period
- The buoyant surface water layer was formed due prolonged melting of glaciers

Correspondence to:
E. S. Kandiano,
ekandiano@geomar.de

A cold and fresh ocean surface in the Nordic Seas during MIS 11: Significance for the future ocean

Evgenia S. Kandiano[1,2], Marcel T. J. van der Meer[1], Henning A. Bauch[3,4], Jan Helmke[2], Jaap S. Sinninghe Damsté[1,5], and Stefan Schouten[1,5]

[1]NIOZ Netherlands Institute for Sea Research, Utrecht University, Den Burg, Netherlands, [2]GEOMAR Helmholtz Centre for Ocean Research Kiel, Kiel, Germany, [3]Alfred Wegener Institute Helmholtz Centre for Polar and Marine Research, Bremerhaven, Germany, [4]GEOMAR Helmholtz Centre for Ocean Research, Kiel, Germany, [5]Department of Earth Sciences, Utrecht University, Utrecht, Netherlands

Abstract Paleoceanographical studies of Marine Isotope Stage (MIS) 11 have revealed higher-than-present sea surface temperatures (SSTs) in the North Atlantic and in parts of the Arctic but lower-than-present SSTs in the Nordic Seas, the main throughflow area of warm water into the Arctic Ocean. We resolve this contradiction by complementing SST data based on planktic foraminiferal abundances with surface salinity changes using hydrogen isotopic compositions of alkenones in a core from the central Nordic Seas. The data indicate the prevalence of a relatively cold, low-salinity, surface water layer in the Nordic Seas during most of MIS 11. In spite of the low-density surface layer, which was kept buoyant by continuous melting of surrounding glaciers, warmer Atlantic water was still propagating northward at the subsurface thus maintaining meridional overturning circulation. This study can help to better constrain the impact of continuous melting of Greenland and Arctic ice on high-latitude ocean circulation and climate.

1. Introduction

Recent paleoclimatic investigations have designated Marine Isotope Stage (MIS) 11 a "super interglacial" due to up to 4°C higher terrestrial temperatures in the Arctic Eurasia in comparison to those of MIS 1 and 5e [*Melles et al.*, 2012; *Vaks et al.*, 2013]. Moreover, marine data indicate at least seasonally ice-free conditions in the western Antarctic sector during this period [*Cronin et al.*, 2013] and significantly warmer-than-present sea surface temperatures (SSTs) in the middle latitudes of the North Atlantic [*de Vernal and Hillaire-Marcel*, 2008; *McManus et al.*, 2003; *Kandiano and Bauch*, 2002, 2007], as well as a remarkably strong Atlantic meridional overturning circulation (AMOC) [e.g., *Vázquez Riveiros et al.*, 2013]. However, puzzling differences arise when comparing foraminifera-based SST reconstructions in the Nordic Seas with those from the Arctic and the middle latitudinal North Atlantic. The planktic foraminiferal compositions, with a strong dominance of the polar species *Neogloboquadrina pachyderma* sinistral (s), imply that the ocean surface layer in the Nordic Seas remained relatively cold during the period of peak interglacial conditions, i.e., MIS 11 sensu stricto (ss), a period lasting from circa 419 to circa 400 ka in this region. A modest increase in the relative abundance of the subpolar Atlantic water indicative species *Turborotalita quinqueloba*, a counterpart of *N. pachyderma* (s) in the Nordic Seas, occurred in this region only toward the end of MIS 11ss. The period of enhanced *T. quinqueloba* abundance coincided with the minimal ice global volume and is defined as a regional climate optimum [*Kandiano et al.*, 2012]. However, the foraminiferal assemblages imply that SSTs during MIS 11ss never reached those of the Holocene [*Bauch*, 1997; *Kandiano et al.*, 2012]. We hypothesized that the unusually cold conditions of the ocean surface during the early interglacial phase of MIS 11ss was caused by prolonged melting of the surrounding ice sources, which delivered freshwater into the Nordic Seas, thereby generating a thick, relatively cold and low salinity, buoyant mixed surface layer [*Kandiano and Bauch*, 2007]. This mixed layer probably was reduced only during the climate optimum as can indirectly be inferred from the abundance increase of *T. quinqueloba*.

To confirm the hypothesis that relatively fresh sea surface waters occupied the Nordic Seas during MIS 11ss and to assess the extent of environmental changes during its climate optimum requires assessing past sea surface salinity (SSS). In this study we reconstructed SSS changes during MIS 11ss (relative to the modern values, ΔSSS) from the hydrogen isotope compositions of long chain alkenones (δD_A) obtained from sediment core MD992277 (the central Nordic Seas). δD_A is a relatively new paleoceanographical proxy which,
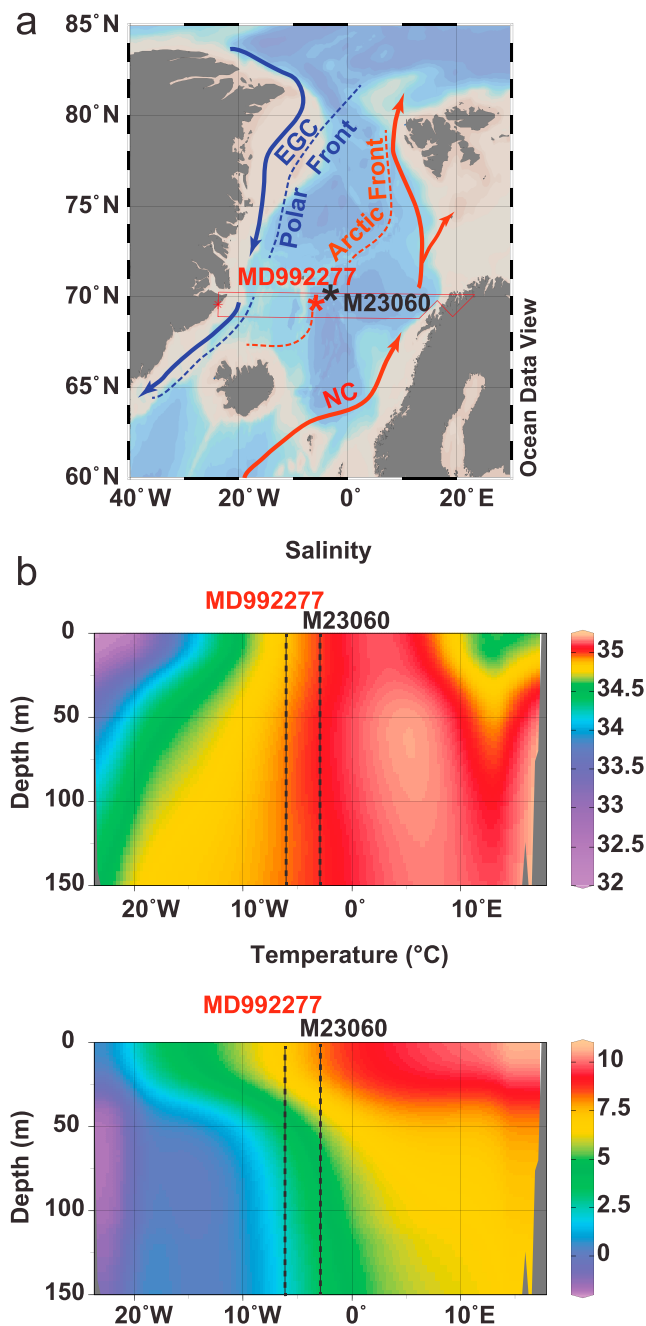
Figure 1. (a) Generalized surface ocean circulation in the Nordic Seas and geographical positions of the investigated core MD992277 (69°15′N, 06°19′W, 2800 m water depth) and reference core M23060 (70°00.10′N, 02°59.70′W, 3229 m water depth). EGC: East Greenland Current and NC: Norwegian Current. Red box indicates transect for temperature and salinity profiles. Red box defines transect of profiles. (b) Temperatures and salinity profiles for the summer season, July–September [*Schlitzer*, 2015; *World Ocean Circulation Experiment*, 2001]. Positions of cores MD992277 and M23060 are indicated by black lines.

contrary to $\delta^{18}O$, bears a salinity signal independent of temperature changes [*Schouten et al.*, 2006; *van der Meer et al.*, 2007, 2008]. The reconstructions of SSS changes were supported by benthic and planktic oxygen isotope measurements, planktic foraminiferal census data, and ice-rafted debris (IRD) counts.

If we are able to prove a presence of the fresh surface layer in the Nordic Seas during MIS 11, then our study may shed light on forthcoming climate development. Results of modeling experiments on a potential AMOC reaction to the fresh water input are contradictory, so far. Some of them showed a highly increased sensitivity of the AMOC strength [e.g., *Hawkins et al.*, 2011; *Brunnabend et al.*, 2015] in response to potential fresh water input, while others demonstrate only a minor effect [e.g., *Ridley et al.*, 2005; *Hu et al.*, 2011].

2. Material and Methods

2.1. Oceanographic Setting

The Nordic Seas are a partially isolated basin fed by the warm and saline Atlantic waters transported by the Norwegian Current (NC) in its eastern part and by the cold and fresh Arctic waters flowing south as the East Greenland Current (EGC) in the west. Accordingly, the oceanographic fronts are aligned in a submeridional direction [*Orvik and Niiler*, 2002]. Modern SST and SSS gradients clearly reflect these contrasting physical properties in the water masses (Figure 1).

Studied sediment core MD992277 was taken from a climatically sensitive area near the Arctic front, where the surface waters represent a mixture of the Arctic and Atlantic derived water masses (Figure 1). Today, this area experiences a direct influence

of Atlantic water advection from the east. During glacial times, however, polar waters expanded far to the south of MD992277 site and into the subpolar North Atlantic. Since a subzonal alignment of the oceanographical fronts was characteristic for MIS 11 [*Bauch*, 1997; *Kandiano et al.*, 2012], paleoceanographical

reconstructions at site MD992277 for this period can resolve the oceanographical situation also in the eastern part of the Nordic Seas where the Atlantic water input presently occurs. In order to enable a comparison of SSS reconstructions between MIS 11ss and the late Holocene, the core top sample of a nearby core M23060 was used as a reference (Figure 1).

2.2. Chronology

The downcore position of MIS 11 in core MD992277 was firmly established by correlating carbonate content and planktic δ^{18}O to those of core PS1243 from the same site [*Helmke et al.*, 2005]. An age model of core PS1243 was established on the basis of planktic foraminiferal δ^{18}O records [*Bauch*, 1997; *Bauch et al.*, 2000]. The age model of core MD992277 was later improved using the benthic δ^{18}O records of *Kandiano et al.* [2012]. The presented study considers the period between 424 and 380 ka which covers the final phase of glacial Termination V (MIS 12), MIS 11ss, and the onset of the ensuing glacial inception.

2.3. Sampling and Sample Preparation

Core MD992277 was sampled continuously as 1 cm thick slices. Organic and inorganic analyses were partly produced on different sample sets, using step intervals between 1 and 3 cm. All samples were freeze-dried prior processing for analyses.

2.4. Hydrogen Isotope Composition of Alkenones and Derived ΔSSS Reconstructions

Samples for δD_A analysis were homogenized and extracted using an Accelerated Solvent Extractor (DIONEX AS E350, 100°C) and a mixture of dichloromethane (DCM): methanol (MeOH, 9:1 vol/vol). The alkenone fractions were obtained by separation of the organic extracts on Al_2O_3 columns using hexane: DCM (9:1 vol/vol), hexane: DCM (1:1 vol/vol), and DCM: MeOH (1:1 vol/vol) with the middle fraction containing the alkenones.

The hydrogen isotopic compositions of the alkenones were determined by a GC/Thermal Conversion/isotope ratio monitoring mass spectrometer using a GC coupled to a Thermo Electron DELTA V mass spectrometer via a GC-isolink and Conflo IV interface. The procedure was described in detail by *Kasper et al.* [2015]. The H_3^+ correction factor was determined daily and varied between 2.81 and 2.93. The δD_A measurements were performed for the combined $C_{37:2}$ and $C_{37:3}$ alkenones following the approach of *van der Meer et al.* [2013]. Standard deviations of the replicate measurements in most cases did not exceed 5‰.

Since besides salinity also global ice volume changes strongly affect δD_A during glacial-interglacial transitions [*Rohling*, 2000], SSS changes were assessed only for the period of climate optimum, i.e., between 409 and 401 ka, when the global ice volume was stable. They were derived from δD_A following generally the approach of *van der Meer et al.* [2007].

First, we calculated δ^{18}O of sea water ($\delta^{18}O_W$) from foraminiferal temperatures (*T*) and δ^{18}O in tests of *N. pachyderma* (s) ($\delta^{18}O_{Np(s)}$) using the equation applicable for low temperatures [*Horibe and Oba*, 1972]:

$$T = 17.04 - 4.34 * \left(\delta^{18}O_{Np(s)} - \delta^{18}O_W\right) + 16 * \left(\delta^{18}O_{Np(s)} - \delta^{18}O_W\right)^2. \tag{1}$$

Then we calculated δD of sea water (δD_W) using the modern Arctic Meteoric Water Line from *Cox* [2010]:

$$\delta D_W = \delta^{18}O_W * 7.37 - 0.72. \tag{2}$$

Subsequently, we calculated SSS (S) using the relationship derived from *Gephyrocapsa oceanica* [*Schouten et al.*, 2006] and the combined data sets of *Emiliania huxleyi* of *Schouten et al.* [2006] and *M'Boule et al.* [2014] (Figure 2) as follows:

$$Gephyrocapsa\ oceanica: \text{S} = (\alpha - 0.676)/0.003 \tag{3}$$

$$Emiliania\ huxleyi: \text{S} = (\alpha - 0.711)/0.0029 \tag{4}$$

where $\alpha = (\delta D_A + 1000)/(\delta D_W + 1000)$. The δD_A values of several sediment samples were averaged in order to obtain synchronous ages with the δ^{18}O data set.

Finally, we adjusted the SSS values obtained for MIS 11ss from core MD992277 to the SSS estimate obtained from the δD values of alkenones in the core top sample of core M23060. The reason for adjustment was that the absolute SSS estimate of core top sample in core M23060 was higher than modern SSS value at
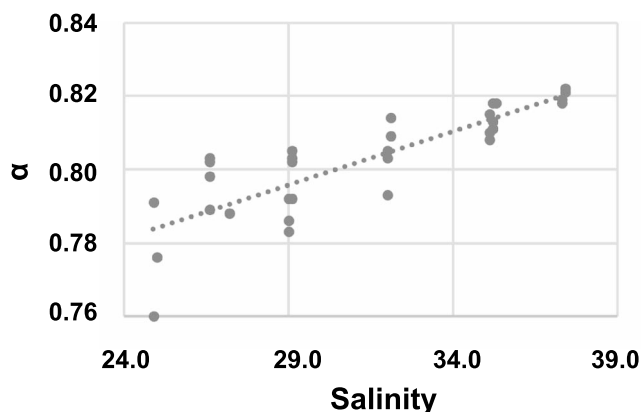
Figure 2. Fractionation factor α of C_{37} alkenones versus water for *E.huxleyi* from the combined data of culture experiments by *Schouten et al.* [2006] and *M'Boule et al.* [2014] plotted against salinity.

the same site (e.g., 38.9 versus 35.1 for *E. huxleyi* equation) [*Boyer et al.*, 2013]. In order to calculate absolute SSS values for the core top sample from core M23060, the $\delta 18O$ value from *Vogelsang* [1990] was used. Therefore, we rely rather on ΔSSS reconstructions than on absolute SSS values. The slopes of the linear regressions describing the relation between salinity and the fractionation factor α between alkenones and water are very similar for *E. huxleyi* and *G. oceanica*. This implies that species composition has a negligible effect on ΔSSS values (Figure 3).

2.5. Foraminiferal Census Counts, Derived Temperature Reconstructions, Benthic and Planktic Oxygen Isotope Analyses, and IRD

Planktic and benthic stable oxygen isotope data, foraminiferal census data, and iceberg-rafted debris (IRD) were published in *Kandiano et al.* [2012]. The summer season (July–September) temperatures for this study were estimated from the foraminiferal census counts for the 0–150 m water depth level using the modern analogue technique (five best analogues; standard deviation of the residuals 1.05) [*Prell*, 1985]. This water layer corresponds to the presumed depth habitat of the modern foraminifers in the polar environment [*Carstens et al.*, 1997]. For calibrations, foraminiferal core top data of *Husum and Hald* [2012] were linked to modern temperatures [*Boyer et al.*, 2013] neglecting a potential difference in foraminiferal proportions between > 80 μm and 100–1000 μm fractions used in this study and by *Husum and Hald* [2012], respectively. The foraminiferal abundances were reduced to only two dominant species following the approach applied in the Arctic region by *Cronin et al.* [2013].
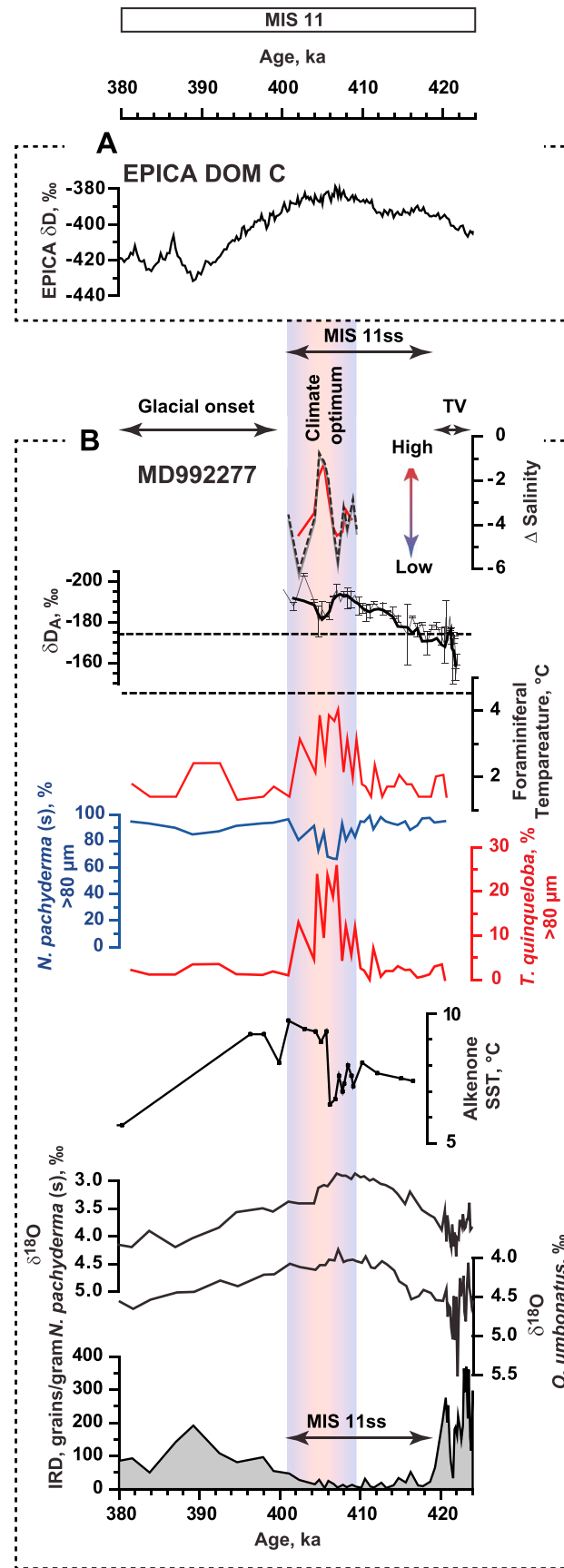
3. Results

3.1. IRD, Planktic, and Benthic Oxygen Isotopes

A large IRD input associated with multiple high-amplitude fluctuations in benthic and planktic foraminiferal $\delta^{18}O$ values is observed during Termination V until 419 ka (Figure 3). In spite of the sharp decrease at 419 ka, IRD deposition did not cease completely but persisted into MIS 11ss implying a continuous iceberg delivery to the site. From circa 419 ka onward both benthic and planktic $\delta^{18}O$ exhibited a gradual decrease reflecting a combined signal of a continued global ice volume decrease, a temperature rise, and, in the planktic record, also a freshwater component. The benthic and planktic $\delta^{18}O$ values arrived at 4.0‰ and 2.9‰, respectively, at circa 409 ka, marking the start of the climate optimum. Surprisingly, after this time the $\delta^{18}O$ records show a diachronous behavior. The benthic $\delta^{18}O$ values show a plateau-like pattern between 409 and 401 ka, clearly marking the period of a stable ice volume and, at the same time, a high sea level stand. The planktic $\delta^{18}O$ record, in contrast, exhibits a plateau-like pattern of much shorter duration, i.e., between 409 and 407 ka, with a sharp increase of 0.5‰ during the following 2 ky. After 401 ka onward both $\delta^{18}O$ records as well as IRD content showed a gradual increase toward glacial values reflecting the onset of a new glaciation. The stratigraphy of MD992277 correlates well with the δD proxy trend (temperature) in Antarctica (Figure 3).

3.2. Planktic Foraminiferal Abundances and Temperatures

During MIS 11ss, planktic foraminiferal assemblages at site MD992277 are dominated by two species: the polar species *N. pachyderma* (s) and the subpolar species *T. quinqueloba* (Figure 3). In contrast to the Holocene, however, *N. pachyderma* (s) remained strongly dominant in the Nordic Seas during the total period of MIS 11 [*Kandiano et al.*, 2012]. In core MD992277 the relative abundance of *T. quinqueloba* remained negligible until 409 ka. This species increased only during the climate optimum, between 409 and 401 ka, with maximal values up to 24% between 407 and 405 ka, which corresponds to a temperature increase from 2

Figure 3. (a) Ice core data from Antarctica, here shown on its own time scale [*European Project for Ice Coring in Antarctica Community Members*, 2004], in comparison with various proxy records from core MD992277 (B; top to down): ΔSSS calculated for *E. huxleyi* (black dash line) and *G. oceanica* (gray line) relative to the SSS reconstructed from the core top sample of core M23060 (note that calculated ΔSSS curves for the two species are almost identical). The colored line represents three-point average; δD_A, grey line with vertical bars represents measurements with standard deviations of duplicate measurements. The black line represents three-point average values; black dotted line represents core top δD_A value of core M23060; Summer temperatures in 0–150 m depth layer reconstructed from planktic foraminiferal abundances, black dotted line represents appropriate modern temperature value at site MD992277; Relative abundance of the polar planktic foraminifer *N. pachyderma* (s) [*Kandiano et al.*, 2012]; Relative abundance of the planktic subpolar foraminifer *T. quinqueloba* [*Kandiano et al.*, 2012]; Alkenone SSTs [*Kandiano et al.*, 2012]; planktic $\delta^{18}O$ derived from *N. pachyderma* (s) [*Helmke et al.*, 2005; *Kandiano et al.*, 2012]; benthic $\delta^{18}O$ derived from *O. umbonatus* [*Kandiano et al.*, 2012]; IRD [*Helmke et al.*, 2005]. MIS 11, MIS 11ss, Termination V (TV), and glacial onset are indicated on the top panel; the climate optimum is marked by a vertical bar.

to 4°C (Figure 3). However, this temperature did not reach the present-day temperature of 4.5°C at this site [*Boyer et al.*, 2013]. In relation to Antarctica, the period of maximal temperatures started about 3 ky earlier, at 412 ka. However, its end coincides at both sites (Figure 3).

3.3. Hydrogen Isotopic Composition of Alkenones and SSS Reconstruction

δD_A showed a progressive decrease from −162‰ to −193‰ between 422 and 409 ka (Figure 3). This matches the period of the global ice volume decrease, which likely contributed substantially to the δD change. Between 409 and 407 ka, when global ice volume reached its minimum and was relatively stable, the δD_A record first reached a plateau and then δD_A values abruptly increased to −183‰ around 405 ka. Since global ice volume was relatively stable at that time, this change implies an SSS increase,

coinciding with the main phase of the proliferation of *T. quinqueloba* (Figure 3). After 404 ka, δD_A returned to values similar to ones before 407 ka.

Although salinity and global ice volume have a strong impact on δD_A value, other factors may also have an influence such as changes in haptophyte species composition [*Schouten et al.*, 2006; *M'Boule et al.*, 2014; *Chivall et al.*, 2014], light intensities [*van der Meer et al.*, 2015] and, to a lesser degree, algal growth rate [*Schouten et al.*, 2006]. It seems unlikely that the change in δD_A between 407 and 404 ka could be the result of a change in growth rate because a more than twofold reduction in growth rates would be required for a 11‰ δD_A increase [*Schouten et al.*, 2006]. Unrealistically strong reduction of light intensities corresponding to 60 μmol photons m^{-2} s^{-1} would also be needed to cause the observed changes in δD_A fractionation [*van der Meer et al.*, 2015]. Furthermore, in natural conditions *E. huxleyi*, for example, form large blooms only at light intensities > 530 μmol photons m^{-2} s^{-1} [*Nanninga and Tyrrell*, 1996], i.e., at the range where fractionation between δD_W and δD_A is constant [*van der Meer et al.*, 2015]. With respect to a species composition, it is not expected that species composition changes in the central Nordic Seas might impact δD_A during MIS 11ss because investigation of coccolith assemblages in core top samples have revealed a reduced diversity in the Nordic Seas due to the severity of the living conditions. It is restricted to only one open ocean alkenone synthesizing species, *E. huxleyi* [*Samtleben and Schröder*, 1992; *Solignac et al.*, 2008]. We should note that during MIS 11 the Nordic Seas were dominated by *G. muellerae* [*Bleil and Gard*, 1989], a close ancestor of *G. oceanica* [*Bollmann*, 1997], while *E. huxleyi* occurred in the Nordic Seas for the first time during MIS 8 descending from Gephyrocapsid ancestor [*McIntyre*, 1970]. We assume that for this ancestor the relation between salinity and fractionation factor α between hydrogen isotopes and water was characterized by a slope similar to the ones revealed during culture experiments of *Schouten et al.* [2006] and *M'Boule et al.* [2014]. Since migrations of oceanographic fronts over site MD992277 during MIS 11 were not registered by previous investigations [*Kandiano et al.*, 2012], seasonal changes in productivity are not expected to influence our salinity reconstructions. Moreover, in the Nordic Seas the coccoliths blooms occur simultaneously with foraminiferal blooms [*Kohfeld et al.*, 1996; *Schröder-Ritzrau et al.*, 2001] with the latter being dependent on food availability. Therefore, the signals of δD_A and foraminiferal δ^{18}O of water are likely formed at the same time. Thus, an influence of all aforementioned factors on δD_A during the climate optimum of MIS 11ss seems negligible. Therefore, the changes in the δD_A during the climate optimum are predominantly ascribed to salinity and δD_w.

ΔSSS reconstructions derived from δD_A analysis show that SSS values at 409 ka correspond to values ~3 lower than the late Holocene SSS reconstructed from the core top sample of core M23060. The change of δD_A between 407 and 405 ka suggests an abrupt and transient increase in SSS by ~2 (Figure 3). However, the highest SSS values registered during MIS 11ss are still ~1 salinity unit lower than the SSS as reconstructed from the core top sample of core M23060. The transient SSS increase during the MIS 11ss climate optimum explains the observed diachronism of benthic and planktic δ^{18}O records during the climate optimum, i.e., the early increase of planktic δ^{18}O values at 407 ka can be attributed to a change in SSS.

4. Paleoceanographical Implications and Conclusions

Our reconstructed ΔSSS record indicates that the ocean surface in the central Nordic Seas was fresher during MIS 11ss than during the late Holocene, as compared to the core top sample from site M23060. In combination with reduced abundances of subpolar foraminifera and lower SST, this implies the presence of a significant, relatively fresh, mixed surface layer. We assume that this relatively fresh mixed layer expanded into the eastern part of the Nordic Seas and as far south as at least 68°N taking into account an absence of oceanographic fronts between site MD992277 and site M23063 (see map Figure 1), respectively [*Kandiano et al.*, 2012]. The resulting increased buoyancy of the surface water in the Nordic Seas during MIS 11ss likely pushed the Atlantic water mass downward. Such a scenario would resolve the controversy between the warm SSTs in the Arctic and the middle latitudes of the North Atlantic and the enigmatically low SSTs in the Nordic Seas [*Kandiano and Bauch*, 2007; *Kandiano et al.*, 2012; *Cronin et al.*, 2013].

A likely source of the freshwater feeding the surface mixed layer of the central Nordic Seas during MIS 11ss were those remnant Greenland glaciers descending down to sea level and releasing icebergs, similar to what is still happening today. Indeed, recent studies indicate intensive melting of Greenland Ice Sheet (GIS) during

MIS 11ss which resulted in deglaciation and a development of a forest vegetation in parts over southern Greenland [*Reyes et al.*, 2014; *de Vernal and Hillaire-Marcel*, 2008], while glacier ice remained at least in central Greenland [*Bierman et al.*, 2014] A specific subzonal configuration of the surface water masses in the Nordic Seas during MIS 11 [*Kandiano et al.*, 2012] would allow the arrival of icebergs only from east central and northeast Greenland to site MD992277. In addition, an increased freshwater export from the Arctic into the Nordic Seas could have occurred due to an enhanced hydrological cycle over Siberia [*Melles et al.*, 2012] which would increase river runoff into the Arctic as well as seasonal ice-free conditions in the western Arctic during this period [*Cronin et al.*, 2013]. This seems conceivable especially taking into account results of modern observations showing an increase of Arctic freshwater transport into the Nordic Seas under a negative North Atlantic Oscillation/Arctic oscillation mode due to a diversion of Eurasian runoff eastward toward the Nordic Seas [*Morison et al.*, 2012]. Furthermore, it has been already shown for the NE Atlantic sector that MIS 11 was characterized by the dominance of a negative-like North Atlantic Oscillation/Arctic oscillation circulation pattern [*Kandiano et al.*, 2012]. The relatively low salinity and, therefore, buoyant surface layer obstructed the propagation of near-surface Atlantic water advection into the central and eastern parts of the Nordic Seas. As a consequence the Atlantic water inflow had to be submerged below the mixed layer. A deeper flowing Atlantic water layer with a relatively high salinity stabilized the vertical water mass structure in the Nordic Seas. Such an oceanographical situation might conceptually resemble the modern situation in the eastern Fram Strait where winter sea ice formation and a close vicinity of the polar waters results in freshening of the ocean surface and a subduction of much saltier Atlantic waters to greater depth [*Schauer et al.*, 2004]. Our foraminiferal data further imply that Atlantic water mass propagation during most of MIS 11ss occurred at depths greater than the depth habitat preferred by *T. quinqueloba*, i.e., ~150 m [*Carstens et al.*, 1997].

It seems also conceivable that this fresh and buoyant layer caused the delay of the climate optimum between the Nordic Seas and other regions. A similar situation, although less pronounced, was already described for the last interglacial period [*Bauch and Kandiano*, 2007]. The Atlantic water layer in the central Nordic Seas shallowed only toward the end of MIS 11ss resulting in increased SSS and SST which allowed for a modest proliferation of *T. quinqueloba*. This all together designates the climate optimum (Figure 3).

Despite the presence of a freshwater cover in the central and eastern Nordic Seas, an intensely active AMOC was suggested for MIS 11 in several studies [e.g., *McManus et al.*, 2003; *Dickson et al.*, 2009; *Vázquez Riveiros et al.*, 2013]. For the Nordic Seas, however, it is difficult to decide where and under which circumstances deep convection could have occurred during MIS 11. It is noteworthy in this respect that MIS 11 in the Nordic Seas was characterized by the near absence of an epibenthic foraminiferal assemblage, including the otherwise very ubiquitous interglacial species *Cibicidoides wuellerstorfi*, but dominated by endobenthic-living species during times of very high surface productivity [*Bauch*, 1997; *Struck*, 1997]. Such conditions would indicate poorly ventilated bottom waters and a rather unusual pelagic-benthic coupling [*Bauch et al.*, 2001]. This notion on the benthic fauna and high surface productivity therefore serves as additional evidence for seasonally ice-covered conditions over large parts of the Nordic Seas. We do not rule out, however, that deep convection may have occurred south of the areas from which records of MIS 11 are presently available.

In conclusion, our findings for interglacial MIS 11 may provide useful information for climate modeling as the present climate amplification in the Arctic region is associated with accelerated melting of GIS [*Rignot et al.*, 2011] and sea ice loss in the Arctic [*Kwok et al.*, 2009] which together is already accounting for notable surface ocean property changes in the subarctic seas [e.g., *Dukhovskoy et al.*, 2016].

References

Bauch, H. A. (1997), Paleoceanography of the North Atlantic Ocean (68°–76°N) during the past 450 ky deduced from planktic foraminiferal assemblages and stable isotopes, in *Contributions to the Micropaleontology and Paleoceanography of the Northern North Atlantic*, *Spec. Publ.*, vol. 5, edited by H. C. Hass and M. A. Kaminski, pp. 83–100, Grzybowski Foundation, Krakow, Poland.

Bauch, H. A., and E. S. Kandiano (2007), Evidence for early warming and cooling in North Atlantic surface waters during the last interglacial, *Paleoceanography*, *22*, PA1201, doi:10.1029/2005PA001252.

Bauch, H. A., H. Erlenkeuser, J. P. Helmke, and U. Struck (2000), A paleoclimatic evaluation of marine oxygen isotope stage 11 in the high-northern Atlantic (Nordic Seas), *Global Planet. Change*, *24*, 27–39, doi:10.1016/s0921-8181(99)00067-3.

Bauch, H. A., U. Struck, and J. Thiede (2001), Planktic and benthic foraminifera as indicators for past ocean changes in surface and deep waters of the Nordic Seas, in *The Northern North Atlantic: A Changing Environment*, edited by P. Schäfer et al., pp. 411–421, Springer, New York.

Bierman, P. R., L. B. Corbett, J. A. Graly, T. A. Neumann, A. Lini, B. T. Crosby, and D. H. Rood (2014), Preservation of a preglacial landscape under the Center of the Greenland Ice Sheet, *Science*, *344*, 402–405, doi:10.1126/science.1249047.

Bleil, U., and G. Gard (1989), Chronology and correlation of Quaternary magnetostratigraphy and nannofossil biostratigraphy in Norwegean-Greenland Sea sedimants, *Geol. Rundsch.*, *78*, 1173–1187, doi:10.1007/BF01829339.

Bollmann, J. (1997), Morphology and biogeography of *Gephyrocapsa* coccoliths in Holocene sediments, *Mar. Micropaleontol.*, *29*, 319–350, doi:10.1016/S0377-8398(96)00028-X.

Boyer, T. P., et al. (2013), World Ocean Database 2013, NOAA Atlas NESDIS 72, S. Levitus, Ed., A. Mishonov, Technical eds., Silver Spring, Md, 209, doi:10.7289/V5NZ85MT.

Brunnabend, S. E., J. Schroter, R. Rietbroek, and J. Kusche (2015), Regional sea level change in response to ice mass loss in Greenland, the West Antarctic and Alaska, *J. Geophys. Res. Oceans*, *120*, 7316–7328, doi:10.1002/2015JC011244.

Carstens, J., D. Hebbeln, and G. Wefer (1997), Distribution of planktic foraminifera at the ice margin in the Arctic (Fram Strait), *Mar. Micropaleontol.*, *29*, 257–269, doi:10.1016/s0377-8398(96)00014-X.

Chivall, D., D. M'Boule, D. Sinke-Schoen, J. S. Sinninghe Damsté, S. Schouten, and M. T. J. van der Meer (2014), The effects of growth phase and salinity on the hydrogen isotopic composition of alkenones produced by coastal haptophyte algae, *Geochim. Cosmochim. Acta*, *140*, 381–390, doi:10.1016/j.gca.2014.05.043.

Cox, K. A. (2010), Stable isotopes as tracers for freshwater fluxes into the North Atlantic, PhD thesis, Southampton, Univ. of Southampton, 163.

Cronin, T. M., L. Polyak, D. Reed, E. S. Kandiano, R. E. Marzen, and E. A. Council (2013), A 600-ka Arctic sea-ice record from Mendeleev Ridge based on ostracodes, *Quat. Sci. Rev.*, *79*, 157–167, doi:10.1016/j.quascirev.2012.12.010.

de Vernal, A., and C. Hillaire-Marcel (2008), Natural variability of Greenland climate, vegetation, and ice volume during the past million years, *Science*, *320*, 1622–1625, doi:10.1126/science.1153929.

Dickson, A. J., C. J. Beer, C. Dempsey, M. A. Maslin, J. A. Bendle, E. L. McClymont, and R. D. Pancost (2009), Oceanic forcing of the Marine Isotope Stage 11 interglacial, *Nat. Geosci.*, *2*, 428–433, doi:10.1038/ngeo527.

Dukhovskoy, D. S., et al. (2016), Greenland freshwater pathways in the sub-Arctic Seas from model experiments with passive tracers, *J. Geophys. Res. Oceans*, *121*, 877–907, doi:10.1002/2015JC011290.

European Project for Ice Coring in Antarctica Community Members (2004), Eight glacial cycles from an Antarctic ice core, *Nature*, *429*, 623–628, doi:10.1038/nature02599.

Hawkins, E., R. S. Smith, L. C. Allison, J. M. Gregory, T. J. Woollings, H. Pohlmann, and B. de Cuevas (2011), Bistability of the Atlantic overturning circulation in a global climate model and links to ocean freshwater transport, *Geophys. Res. Lett.*, *38*, L16699, doi:10.1029/2011GL048997.

Helmke, J. P., H. A. Bauch, U. Rohl, and A. Mazaud (2005), Changes in sedimentation patterns of the Nordic Seas region across the mid-Pleistocene, *Mar. Geol.*, *215*, 107–122, doi:10.1016/j.margeo.2004.12.006.

Horibe, Y., and T. Oba (1972), Temperature scales of aragonite water and calcite water systems, *Fossils*, *23*, 69–79.

Hu, A., G. A. Meehl, W. Han, and J. Yin (2011), Effect of the potential melting of the Greenland Ice Sheet on the Meridional Overturning Circulation and global climate in the future, *Deep Sea Res., Part II*, *58*, 1914–1926, doi:10.1016/j.dsr2.2010.10.069.

Husum, K., and M. Hald (2012), Arctic planktic foraminiferal assemblages: Implications for subsurface temperature reconstructions, *Mar. Micropaleontol.*, *96–97*, 38–47, doi:10.1016/j.marmicro.2012.07.001.

Kandiano, E. S., and H. A. Bauch (2002), Implications of planktic foraminiferal size fractions for the glacial-interglacial paleoceanography of the polar North Atlantic, *J. Foraminiferal Res.*, *32*, 245–251, doi:10.2113/32.3.245.

Kandiano, E. S., and H. A. Bauch (2007), Phase relationship and surface water mass change in the NorthEast Atlantic during Marine Isotope stage 11 (MIS 11), *Quat. Res.*, *68*, 445–455, doi:10.1016/j.yqres.2007.07.009.

Kandiano, E. S., H. A. Bauch, K. Fahl, J. P. Helmke, U. Rohl, M. Perez-Folgado, and I. Cacho (2012), The meridional temperature gradient in the eastern North Atlantic during MIS 11 and its link to the ocean-atmosphere system, *Palaeogeogr. Palaeoclimatol. Palaeoecol.*, *333*, 24–39, doi:10.1016/j.palaeo.2012.1003.1005.

Kasper, S., M. T. J. van der Meer, I. S. Castaneda, R. Tjallingii, G.-J. A. Brummer, J. S. Sinninghe Damsté, and S. Schouten (2015), Testing the alkenone D/H ratio as a paleo indicator of sea surface salinity in a coastal ocean margin (Mozambique Channel), *Org. Geochem.*, *78*, 62–68, doi:10.1016/j.orggeochem.2014.10.011.

Kohfeld, K. E., R. G. Faibanks, S. L. Smith, and I. D. Walsh (1996), *Neogloboquadrina pachyderma* (sinistral coiling) as paleoceanographic tracers in polar oceans: Evidence from Northeast Water Polynya tows, sediment traps, and surface sediments, *Paleoceanography*, *11*, 679–699, doi:10.1029/96PA02617.

Kwok, R., G. F. Cunningham, M. Wensnahan, I. Rigor, H. J. Zwally, and D. Yi (2009), Thinning and volume loss of the Arctic Ocean sea ice cover: 2003–2008, *J. Geophys. Res.*, *114*, C07005, doi:10.1029/2009JC005312.

M'Boule, D., D. Chivall, D. Sinke-Schoen, J. S. Sinninghe Damste, S. Schouten, and M. T. J. van der Meer (2014), Salinity dependent hydrogen isotope fractionation in alkenones produced by coastal and open ocean haptophyte algae, *Geochim. Cosmochim. Acta*, *130*, 126–135, doi:10.1016/j.gca.2014.01.029.

McIntyre, A. (1970), *Gephyrocapsa protohuxleyi* sp. n. as possible phyletic link and index fossil for the Pleistocene, *Deep-Sea Res.*, *17*, 187–190, doi:10.1016/0011-7471(70)90097-5.

McManus, J., D. Oppo, J. Cullen, and S. Healey (2003), Marine Isotope Stage 11 (MIS 11): Analog for Holocene and future climate?, in *Earth's Climate and Orbital Eccentricity: The Marine Isotope Stage 11 Question*, *Monogr. Ser.*, vol. 137, edited by A. W. Droxler, R. Z. Poore, and L. Burckle, pp. 69–85, AGU, Washington, D. C.

Melles, M., et al. (2012), 2.8 million years of Arctic climate change from Lake El'gygytgyn, NE Russia, *Science*, *337*, 315–320, doi:10.1126/science.1222135.

Morison, J., R. Kwok, C. Peralta-Ferriz, M. Alkire, I. Rigor, R. Andersen, and M. Steele (2012), Changing Arctic Ocean freshwater pathways, *Nature*, *481*, 66–70, doi:10.1038/nature10705.

Nanninga, H. J., and T. Tyrrell (1996), Importance of light for the formation of algal blooms by *Emiliania huxleyi*, *Mar. Ecol. Prog. Ser.*, *136*, 195–203, doi:10.3354/meps136195.

Orvik, K. A., and P. Niiler (2002), Major pathways of Atlantic water in the northern North Atlantic and Nordic Seas toward Arctic, *Geophys. Res. Lett.*, *19*(19), 1896, doi:10.1029/2002GL015002.

Prell, W. L. (1985), The stability of low latitude sea surface temperatures: An evaluation of the CLIMAP reconstruction with emphasis on positive SST anomalies, U.S. Dept. of Energy, Rep. TR 025, 60.

Reyes, A. V., A. E. Carlson, B. L. Beard, R. G. Hatfield, J. S. Stoner, K. Winsor, B. Welke, and D. J. Ullman (2014), South Greenland ice-sheet collapse during Marine Isotope Stage 11, *Nature*, *510*, 525–528, doi:10.1038/nature13456.

Ridley, J. K., P. Huybrechts, J. M. Gregory, and J. A. Lowe (2005), Elimination of the Greenland ice sheet in a high CO$_2$ climate, *J. Clim.*, *18*, 3409–3427, doi:10.1175/jcli3482.1.

Rignot, E., I. Velicogna, M. R. van den Broeke, A. Monaghan, and J. Lenaerts (2011), Acceleration of the contribution of the Greenland and Antarctic ice sheets to sea level rise, *Geophys. Res. Lett.*, *38*, L05503, doi:10.1029/2011GL046583.

Rohling, E. J. (2000), Paleosalinity: Confidence limits and future applications, *Mar. Geol.*, *163*, 1–11, doi:10.1016/s0025-3227(99)00097-3.

Samtleben, C., and A. Schröder (1992), Living coccolithophore communities in the Norwegian-Greenland Sea and their record in sediments, *Mar. Micropaleontol.*, *19*(4), 333–354, doi:10.1016/0377-8398(92)90037-k.

Schauer, U., E. Fahrbach, S. Osterhus, and G. Rohardt (2004), Arctic warming through the Fram Strait: Oceanic heat transport from 3 years of measurements, *J. Geophys. Res.*, *109*, C06026, doi:10.1029/2003JC001823.

Schlitzer, R. (2015), Ocean Data View, odw.awi.de.

Schouten, S., J. Ossebaar, K. Schreiber, M. V. M. Kienhuis, G. Langer, A. Benthien, and J. Bijma (2006), The effect of temperature, salinity and growth rate on the stable hydrogen isotopic composition of long chain alkenones produced by *Emiliania huxleyi and Gephyrocapsa oceanica*, *Biogeosciences*, *3*, 113–119, doi:10.5194/bg-3-113-2006.

Schröder-Ritzrau, A., H. Andruleit, S. Jensen, C. Samtleben, P. Schäfer, J. Matthiessen, H. C. Hass, A. Kohly, and J. Thiede (2001), Distribution, export and alteration of Fossilizable Plankton in the Nordic Seas, in *The Northern North Atlantic: A Changing Environment*, edited by P. Schäfer et al., pp. 81–104, Springer, Berlin.

Solignac, S., A. de Vernal, and J. Giraudeau (2008), Comparison of coccolith and dinocyst assemblages in the northern North Atlantic: How well do they relate with surface hydrography?, *Mar. Micropaleontol.*, *68*, 115–135, doi:10.1016/j.marmicro.2008.01.001.

Struck, U. (1997), Paleoecology of benthic foraminifera in the Norwegian-Greenland Sea during the past ka, in *Contributions to the Micropaleontology and Paleoceanography of the Northern North Atlantic*, *Spec. Publ.*, edited by H. C. Hass and M. A. Kaminski, pp. 51–82, Grzybowski Foundation, Krakow, Poland.

Vaks, A., O. S. Gutareva, S. F. M. Breitenbach, E. Avirmed, A. J. Mason, A. L. Thomas, A. V. Osinzev, A. M. Kononov, and G. M. Henderson (2013), Speleothems reveal 500,000-year history of Siberian permafrost, *Science*, *340*, 183–186, doi:10.1126/science.1228729.

van der Meer, M. T. J., M. Baas, W. I. C. Rijpstra, G. Marino, E. J. Rohling, J. S. Sinninghe Damste, and S. Schouten (2007), Hydrogen isotopic compositions of long-chain alkenones record freshwater flooding of the Eastern Mediterranean at the onset of sapropel deposition, *Earth Planet. Sci. Lett.*, *262*, 594–600, doi:10.1016/j.epsl.2007.08.014.

van der Meer, M. T. J., F. Sangiorgi, M. Baas, H. Brinkhuis, J. S. Sinninghe Damste, and S. Schouten (2008), Molecular isotopic and dinoflagellate evidence for late Holocene freshening of the Black Sea, *Earth Planet. Sci. Lett.*, *267*, 426–434, doi:10.1016/j.epsl.2007.12.001.

van der Meer, M. T. J., A. Benthien, J. Bijma, S. Schouten, and J. S. Sinninghe Damste (2013), Alkenone distribution impacts the hydrogen isotopic composition of the C-37:2 and C-37:3 alkan-2-ones in Emiliania huxleyi, *Geochim. Cosmochim. Acta*, *111*, 162–166, doi:10.1016/j.gca.2012.10.041.

van der Meer, M. T. J., A. Benthien, K. L. French, E. Epping, I. Zondervan, G.-J. Reichart, J. Bijma, J. S. Sinninghe Damste, and S. Schouten (2015), Large effect of irradiance on hydrogen isotope fractionation of alkenones in *Emiliania huxleyi*, *Geochim. Cosmochim. Acta*, *160*, 16–24, doi:10.1016/j.gca.2015.03.024.

Vázquez Riveiros, N., C. Waelbroeck, L. Skinner, J. C. Duplessy, J. F. McManus, E. S. Kandiano, and H. A. Bauch (2013), The "MIS 11 paradox" and ocean circulation: Role of millennial scale events, *Earth Planet. Sci. Lett.*, *371*, 258–268, doi:10.1016/j.epsl.2013.03.036.

Vogelsang, E. (1990), Paläo-Ozeanographie des Europäischen Nordmeeres anhand stabiler Kohlenstoff- und Sauerstoffisotope, Report SFB 313 Kiel Univ. 23, 136.

World Ocean Circulation Experiment (2001), [Available at http://odv.awi.de/en/data/ocean/world_ocean_atlas_2001/.]